Hypertension in mice lacking the proatrial natriuretic peptide convertase corin

Joyce C. Y. Chan*, Ole Knudson, Faye Wu, John Morser, William P. Dole, and Qingyu Wu*

Berlex Biosciences, Richmond, CA 94804

Edited by Maurice B. Burg, National Institutes of Health, Bethesda, MD, and approved November 29, 2004 (received for review September 29, 2004)

Atrial natriuretic peptide (ANP) is a cardiac hormone that regulates blood pressure. In cardiomyocytes, the hormone is synthesized as a precursor, proatrial natriuretic peptide (pro-ANP), which is proteolytically converted to active ANP. Corin is a cardiac transmembrane serine protease that has been shown to process pro-ANP *in vitro*, but its physiological importance had not been established. Here, we show that corin-deficient ($Cor^{-/-}$) mice develop normally during embryogenesis and survive to postnatal life. $Cor^{-/-}$ mice have elevated levels of pro-ANP but no detectable levels of ANP as compared with WT littermates. Infusion of an active recombinant soluble corin transiently restores pro-ANP conversion, resulting in the release of circulating biologically active ANP. Using radiotelemetry to assess blood pressure, we find that $Cor^{-/-}$ mice have spontaneous hypertension as compared with WT mice, and it is enhanced after dietary salt loading. Pregnant $Cor^{-/-}$ mice demonstrate late-gestation proteinuria and enhanced high blood pressure during pregnancy. In addition, $Cor^{-/-}$ mice exhibit cardiac hypertrophy resulting in a mild decline in cardiac function later in life. Thus, our data establish corin as the physiological pro-ANP convertase and indicate that corin deficiency may contribute to hypertensive heart disease.

blood pressure | cardiac hypertrophy | preeclampsia | serine protease

Atrial natriuretic peptide (ANP) is a peptide hormone synthesized in the heart as an inactive precursor, proatrial natriuretic peptide (pro-ANP), which is stored in the dense granules of cardiomyocytes. In response to volume expansion and pressure overload, pro-ANP is secreted from cardiomyocytes and proteolytically cleaved, converting it to the mature peptide, ANP. In target organs such as kidney and blood vessels, ANP stimulates production of intracellular cGMP in a receptor-dependent manner, leading to natriuresis, diuresis, and vasodilatation, thereby decreasing blood pressure through reduction of intravascular volume and systemic vascular resistance (for review, see ref. 1). Despite the importance of the ANP-mediated pathway in regulating blood pressure and body fluid homeostasis, the enzyme(s) responsible for pro-ANP conversion remained poorly defined.

Corin is a type II transmembrane serine protease highly expressed in the heart (2–4). Cell-based studies have shown that recombinant human corin converts pro-ANP to active ANP in a sequence-specific manner (5, 6). More recently, purified recombinant human corin also has been shown to process pro-ANP (7), indicating that corin is likely the pro-ANP convertase. Because other proteases such as thrombin and kallikrein have also been reported to cleave pro-ANP *in vitro* (8, 9), it remained to be demonstrated whether corin indeed is the physiological pro-ANP convertase.

To define the biological role of corin, we generated corin-deficient mice ($Cor^{-/-}$) by homologous recombination. Our results show that pro-ANP conversion was abolished in these mice. $Cor^{-/-}$ mice develop hypertension that is further enhanced by high-salt diet and during pregnancy. These data show that corin is a physiological pro-ANP convertase and plays a critical role in maintaining normal blood pressure.

Materials and Methods

Generation of $Cor^{-/-}$ Mice. The targeting vector contained both *neomycin phosphotransferase* (neo^R) and *thymidine kinase* (*TK*) genes driven by the PGK promoter. The neo^R gene, placed in the opposite orientation to *corin* transcription, was flanked by 1.5- and 5.9-kb segments adjacent to exon 19 (Fig. 1*a*). The targeting vector was transfected into 129/SvJ RW4 embryonic stem cells by electroporation. Positive cell lines were selected and injected into embryonic age 3.5 days post coitum C57BL6 blastocysts, followed by implantation into pseudopregnant females to generate chimeric mice. These mice were then crossbred with C57BL6 females to obtain germline transmission of the mutated allele.

Corin genotypes were determined by PCR by using three primers simultaneously to detect both WT and mutant *corin* alleles: PF, a sequence external to the 5′ region (5′-CAGAACTCTGAGTGACAGGC-3′); PB1 from intron 18 (5′-TGTCCCTTAGGTGATGATCC-3′), which would be deleted upon homologous recombination; and PB2 from the neo^R gene (5′-TGCTTTACGGTATCGCCGCT-3′). Amplification of WT and mutant alleles produced ≈1.5- and ≈2-kb fragments, respectively. The data were confirmed by Southern analysis of *Bam*HI-digested genomic DNA by using a 377-bp cDNA probe derived from a region upstream of the 5′ homologous region. A 4-kb hybridizing band indicated the mutant allele, whereas a 2-kb band indicated the WT allele.

RNA Analysis. mRNA was isolated from heart tissue by using the FastTrack 2.0 mRNA kit (Invitrogen). Northern analysis of corin mRNA expression was performed by using [^{32}P]-dCTP-labeled probes for corin and β-actin by using standard techniques.

Analysis of Molecular Forms of ANP. Mouse atrial extracts or control synthetic ANP (Bachem) were separated by RP-HPLC by using a C-18 column (4.6 × 250 mm; Phenomenex, Torrance, CA), equilibrated in 0.1% trifluoroacetic acid (TFA) and eluted with a 20–50% acetonitrile gradient in TFA. Fractions were concentrated and assessed for the presence of pro-ANP and ANP by Western analysis by using a rabbit anti-ANP polyclonal antibody (Peninsula Laboratories). Pro-ANP and ANP were quantified by using an enzyme immunoassay (SPIBio, Massy, France).

Restitution of *in Vivo* pro-ANP Conversion and Assay for cGMP-Stimulating Activity. The generation, purification, and characterization of recombinant soluble corin, EKsolCorin, are described in ref. 7. Blood was sampled 1 h after tail-vein injection of EKsolCorin (3 mg/kg) or control vehicle. To assess the cGMP-stimulating activity of ANP, baby hamster kidney cells were grown in 96-well plates in MEM medium supplemented with

This paper was submitted directly (Track II) to the PNAS office.

Abbreviations: ANP, atrial natriuretic peptide; $Cor^{-/-}$, corin deficient; DBP, diastolic blood pressure; LV, left ventricular; MAP, mean arterial pressure; neo^R, neomycin phosphotransferase; NPRA, natriuretic peptide receptor A; pro-ANP, proatrial natriuretic peptide; SBP, systolic blood pressure.

*To whom correspondence may be addressed. E-mail: joycecy_chan@yahoo.com or qywu88@yahoo.com.

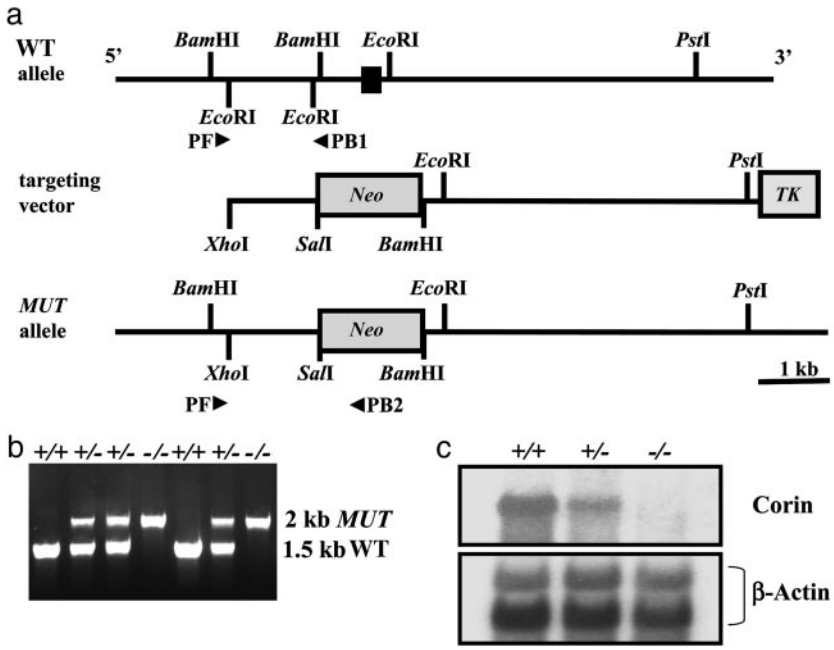

Fig. 1. Targeted disruption of the mouse *corin* gene. (*a*) Structure of the mouse *corin* gene in proximity of, and including, exon 19 (filled bar). The targeting vector contained *neo*^{R} and *thymidine kinase (TK)* genes, both driven by the PGK promoter. The *neo*^{R} gene, in opposite orientation to *corin* transcription, was flanked by a 1.5-kb fragment 5′, and a 5.9-kb fragment 3′ of exon 19. Restriction enzymes used for cloning and Southern hybridization are shown. Primers used for genotyping (PF, PB1, and PB2) are shown (arrowheads). The predicted mutant (*MUT*) allele is shown. (*b*) PCR amplification of genomic DNA with primers PF and PB1 gave rise to an ≈1.5-kb fragment representing the WT allele, whereas primers PF and PB2 amplified an ≈2-kb fragment representing the *MUT* allele. (*c*) Northern hybridization identified *corin* transcripts in cardiac tissues from WT and *Cor*$^{+/-}$ but not *Cor*$^{-/-}$ mice. Levels in *Cor*$^{+/-}$ were ≈50% less than those in WT. The same blot was reprobed by using a β-actin cDNA probe as a control for RNA sample loading.

10% FBS and 1% L-glutamine. Confluent cells were washed once with serum-free medium and incubated with diluted plasma samples at 37°C for 10 min. After lysis of the cells, intracellular cGMP concentration was determined with the Biotrak EIA kit, as described in ref. 6. Each experimental condition was assayed in quadruplicate.

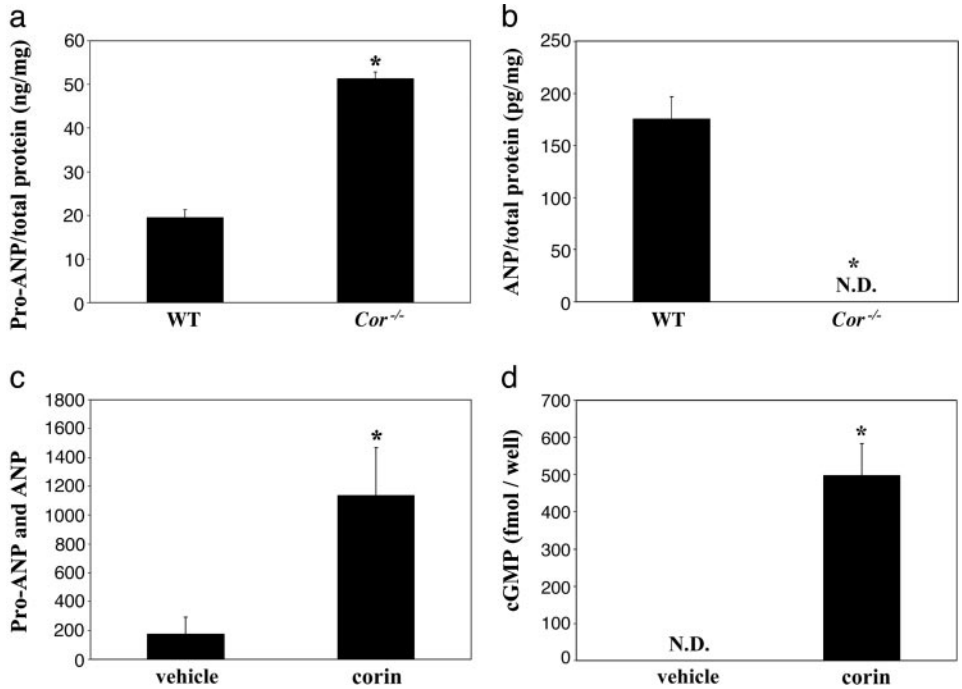

Fig. 2. Pro-ANP and ANP levels in *Cor*$^{-/-}$ mice. Pro-ANP (*a*) and ANP (*b*) levels in atrial extracts from WT and *Cor*$^{-/-}$ mice were determined by HPLC, Western, and ELISA analyses, as described in *Materials and Methods*. (*c*) i.v. injection of EKsolCorin in *Cor*$^{-/-}$ mice results in a significant transient increase in total plasma pro-ANP and ANP antigen levels as compared with injection with vehicle. (*d*) A concomitant increase in plasma ANP activity was observed, as measured by a cell-based cGMP-stimulating activity assay. *, $P < 0.01$ vs. WT or vehicle-treated controls, by Student's *t* test. ND, not detectable.

Urine Chemistry. Urine samples were collected by cystocentesis and analyzed for total protein concentration (Idexx Laboratories, Sacramento, CA).

Blood Pressure Measurements. Mice were chronically instrumented in the left common carotid artery with a TA11PA-C20 blood pressure and heart rate telemetry device (DataSciences, Arden Hills, MN) (10). Singly caged under normal environmental conditions in 12-h light/dark cycles, mice were fed with standard diet (0.75% NaCl) or high-salt diet (8% NaCl) and water *ad libitum*. Telemetry receivers (model RPC-1) were placed under individual cages for data acquisition by using A.R.T. Analog data acquisition (DataSciences) and recording systems (Notocord, Kalamazoo, MI). Systolic blood pressure (SBP) and diastolic blood pressure (DBP) were measured for each cardiac cycle over a 24-h time period, and mean arterial pressure (MAP) and heart rate were derived from these measurements.

Transthoracic Echocardiography. Mice were anesthetized with isoflurane, and echocardiograms were obtained by using a SONOS 5500 imaging system (Philips Medical Systems, Besl, The Netherlands), equipped with a 15 MHz imaging transducer (15–6L). Two-dimensional targeted M-mode imaging was obtained from the short-axis view at the level of the largest left ventricular diameter. End-diastolic and end-systolic frames for long-axis and short-axis fractional area change and left ventricular (LV) mass were measured. M-mode measurements of LV end-diastolic diameter, LV end-systolic diameter, and LV anterior- and posterior-wall thickness were made from digital images by using the leading-edge convention of the American Society of Echocardiography. Three to five beats were averaged for each measurement. End diastole was determined from the onset of the QRS complex on the electrocardiogram, and end systole was taken at the peak of posterior-wall motion.

Histology. Mice were anesthetized with a ketamine/xylazine mixture and perfused with saline through the abdominal aorta. After total exsanguination, mice were perfused with Fix J [4% paraformaldehyde/3% sucrose/0.1 M phosphate buffer (pH 7.3)]. Tissues were excised, fixed in Fix J, dehydrated, and embedded in paraffin. Organs were sectioned at 5 μm and stained with hematoxylin and eosin, Masson's Trichrome, or Periodic Acid Schiff stains. Computer-assisted measurement (AXIOVISION 4.2) at 400× magnification was used to determine the diameter of ≈100 individual cardiomyocytes in the left ventricle of each mouse. All measurements were made in a blinded fashion.

Statistical Analysis. Results are shown as means ± SEM. Single comparisons of the mean values were performed by Student's *t* test. Multiple comparisons of mean values were performed by ANOVA, and when found significant, followed by least square difference analysis. Differences were considered to be statistically significant when the *P* value was <0.05. Statistical analysis was performed with STATISTICA software (StatSoft, Tulsa, OK).

Results

Generation of *Cor*$^{-/-}$ Mice. *Cor*$^{-/-}$ mice were generated by deleting exon 19 of the mouse *corin* gene, which encodes both the activation cleavage site and the catalytic histidine residue of the protease domain (Fig. 1*a*). Gene targeting was confirmed by PCR (Fig. 1*b*) and Southern hybridization (data not shown). The lack of corin gene expression in *Cor*$^{-/-}$ mice was verified by Northern analysis by using cDNA probes spanning both 5′ and 3′ regions (Fig. 1*c*). Genotyping of >500 pups from heterozygous (*Cor*$^{+/-}$) matings identified *Cor*$^{-/-}$ mice at the expected Mendelian frequency. All phenotypic analysis was performed in mice with a genetic background of C57BL6 × 129SvJ (50:50) by using WT littermates as controls. *Cor*$^{-/-}$ mice appeared normal and were fertile but exhibited increased body weight when compared with WT mice, beginning at 15 weeks in females (26.8 ± 0.3 (*n* = 16) vs. 23.3 ± 0.3 g (*n* = 11), $P < 0.05$) and 20 weeks in males (37.7 ± 1.2 (*n* = 19) vs. 33.8 ±

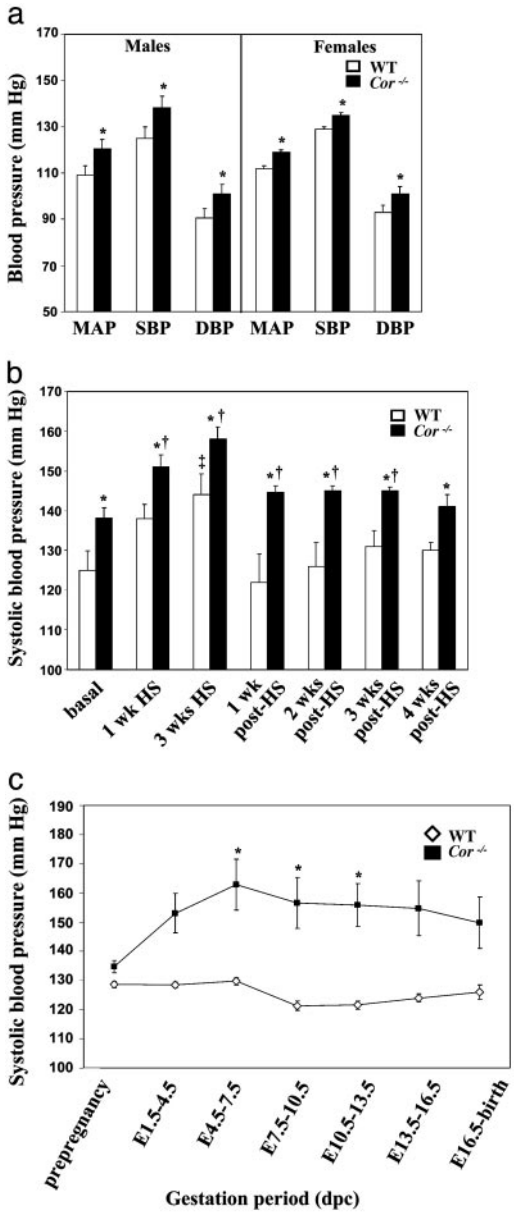

Fig. 3. Hypertension in *Cor*$^{-/-}$ mice. (*a*) When fed with a standard salt diet, *Cor*$^{-/-}$ mice (filled bars) demonstrated elevated blood pressure compared with WT mice (open bars). The data represent averages over 12-h dark/light cycles. $n = 5$ for each genotype and sex. *, $P < 0.01$ vs. WT in the same group, by Student's *t* test. (*b*) SBP increased further in *Cor*$^{-/-}$ mice with 3 weeks of high dietary salt (HS). SBP increased in WT mice but never reached the levels in *Cor*$^{-/-}$ mice treated similarly. After reverting to standard diet (post-HS), SBP normalized in WT mice within 1 week but remained higher in *Cor*$^{-/-}$ mice even after 3 weeks of normal diet. $n = 5$ for each genotype. *, $P < 0.05$ when comparing *Cor*$^{-/-}$ mice to similarly fed WT mice at the same time point; †, $P < 0.05$ when comparing *Cor*$^{-/-}$ mice to *Cor*$^{-/-}$ mice fed with standard diet; ‡, $P < 0.05$ when comparing with WT mice fed with standard diet. Statistical analysis was performed by using ANOVA and least square difference. (*c*) Blood pressure measurement after impregnation showed further increased SBP in *Cor*$^{-/-}$ female mice during pregnancy (■). SBP returned to prepregnancy levels by late gestation or at birth in both genotypes. No significant changes in SBP were observed in WT (◇). *, $P < 0.05$ when comparing pregnant *Cor*$^{-/-}$ mice with *Cor*$^{-/-}$ mice. dpc, days post coitum. Statistical analysis was performed by using ANOVA and least square difference.

Table 1. Cardiac dimensions and function in males at various ages

	n	LVEDD, mm	LVESD, mm	LV mass, mg	LV mass/BW, mg/g	IVS, mm	PW, mm	HR, bpm	FS, %
				12 weeks					
WT	4	4.4 ± 0.1	2.7 ± 0.1	92 ± 5	2.7 ± 0.1	0.91 ± 0.05	0.91 ± 0.15	307 ± 24	38 ± 3
Cor$^{-/-}$	6	4.4 ± 0.2	2.7 ± 0.2	114 ± 5*	3.2 ± 0.2†	0.95 ± 0.06	0.91 ± 0.08	268 ± 15	39 ± 3
				35 weeks					
WT	8	4.6 ± 0.2	2.7 ± 0.2	112 ± 7	3.0 ± 0.2	0.80 ± 0.03	0.81 ± 0.03	329 ± 14	41 ± 2
Cor$^{-/-}$	11	4.6 ± 0.1	2.9 ± 0.1	133 ± 6†	3.1 ± 0.2	0.83 ± 0.03	0.85 ± 0.03	337 ± 13	36 ± 2†

*, $P < 0.01$ versus WT mice in the same age group, Student's *t* test; †, $P < 0.05$. The number of animals is in parentheses. LVEDD, LV end diastolic dimension; LVESD, LV end-systolic dimension; BW, body weight; IVS, interventricular septum; PW, posterior wall thickness; HR, heart rate; bpm, beats per minute; FS, fractional shortening.

1.0 g ($n = 12$), $P < 0.05$). No edema was observed. In *Cor*$^{-/-}$ mice up to 8 months old, no histologic abnormalities were observed in the kidney, liver, spleen, lung, and brain.

Lack of Pro-ANP Processing in *Cor*$^{-/-}$ Mice. To assess the effects of corin deficiency on pro-ANP processing, atrial extracts were prepared from WT and *Cor*$^{-/-}$ mice and subjected to RP-HPLC, Western analysis, and ELISA to isolate and quantify pro-ANP and ANP. Levels of pro-ANP were 2.6-fold higher in *Cor*$^{-/-}$ mice compared with that in WT mice (Fig. 2*a*), whereas ANP was undetectable in *Cor*$^{-/-}$ mice (Fig. 2*b*). i.v. injection of EKsolCorin (7), an active recombinant soluble corin, resulted in a significant increase in circulating antigen levels of pro-ANP and ANP, as measured by an ELISA-based assay that detects both pro-ANP and ANP (Fig. 2*c*). A significant increase of active ANP in plasma was confirmed by a cGMP-stimulating activity assay (6) (Fig. 2*d*). As a control, injection with vehicle alone did not generate any detectable ANP activity (Fig. 2*d*), indicating that the low antigen level detected in the same plasma samples was pro-ANP (Fig. 2*c*). Thus, pro-ANP conversion could be transiently restored with injection of an active soluble corin in *Cor*$^{-/-}$ mice.

Spontaneous and Salt-Sensitive Hypertension in *Cor*$^{-/-}$ Mice. The ANP-mediated pathway plays an important role in regulating blood pressure. We used indwelling telemetry in nonrestrained, nonanesthetized mice to assess the effect of corin deficiency on blood pressure. *Cor*$^{-/-}$ mice fed normal chow diet showed significant increases in MAP compared with WT in males [120 ± 3 vs. 109 ± 4 mmHg (1 mmHg = 133 Pa), $P < 0.05$] and females (119 ± 2 vs. 112 ± 1 mmHg, $P < 0.02$), resulting from increases in both SBP and DBP (Fig. 3*a*). No differences were observed in heart rate. SBP was elevated further with dietary salt loading (Fig. 3*b*). Similar changes in SBP were also observed in WT mice, but their blood pressures never reached the level observed in *Cor*$^{-/-}$ mice (Fig. 3*b*). DBP in *Cor*$^{-/-}$ mice also was increased with the salt diet but did not reach statistical significance when compared with that in similarly treated WT mice (data not shown). SBP returned to presalt levels after reintroduction of normal salt diet, but the time course was longer in *Cor*$^{-/-}$ mice (3–5 weeks) compared with that in WT mice (1 week) (Fig. 3*b*).

Hypertension is Exacerbated During Pregnancy. Corin mRNA expression was detected by *in situ* hybridization in the uterus of pregnant mice but not normal mice (2), suggesting a possible role of corin in pregnancy. We examined blood pressure in *Cor*$^{-/-}$ females throughout the course of pregnancy. Although corin deficiency did not affect fertility, maternal survival, or litter size, longitudinal monitoring of blood pressure after timed mating showed that SBP (Fig. 3*c*), but not DBP (data not shown), was significantly increased in *Cor*$^{-/-}$ mice during pregnancy. SBP returned to prepregnancy levels after birth (data not shown). In contrast, WT mice did not exhibit similar increases but instead had lower SBP during mid-gestation (Fig. 3*c*). Histologic examination of renal sections from late-gestation females revealed no significant differences between WT and *Cor*$^{-/-}$ mice (data not shown). Urinalysis showed significant proteinuria in *Cor*$^{-/-}$ mice at late gestation stages compared with pregnant WT mice (422 ± 126 vs. 184 ± 56 mg/dl, $P = 0.05$), nonpregnant *Cor*$^{-/-}$ mice (156 ± 33 mg/dl, $P < 0.05$), and nonpregnant WT mice (218 ± 50 mg/dl, $P < 0.05$).

Cardiac Hypertrophy in *Cor*$^{-/-}$ Mice. We also assessed cardiac dimensions in male *Cor*$^{-/-}$ mice by two-dimensional transthoracic echocardiography (Table 1) and direct measurements of heart weight (Fig. 4). Cardiac function was also examined by echocardiography (Table 1). Because of the difference in body weight beginning at ≈20 weeks of age, younger animals (12 weeks) were first evaluated. Male *Cor*$^{-/-}$ mice exhibited increased LV mass, but no differences in LV end-diastolic or -systolic dimensions or in interventricular septum or posterior wall thickness. Cardiac function, assessed as velocity of circumferential fiber shortening, fractional area change, and percent fractional shortening, were unaffected. However, by 35 weeks of age, *Cor*$^{-/-}$ mice demonstrated significant decreases in percent fractional shortening compared with WT mice. To ensure that there was no analytical bias in our comparisons, we also evaluated animals of similar weight (≈35 g), regardless of age. Differences in LV mass/body weight were maintained (3.6 ± 0.2 vs. 2.9 ± 0.1 mg/g in WT, $P < 0.01$) by using this method of analysis. Consistent with our data from radiotelemetry, no differences in heart rate were observed between the two

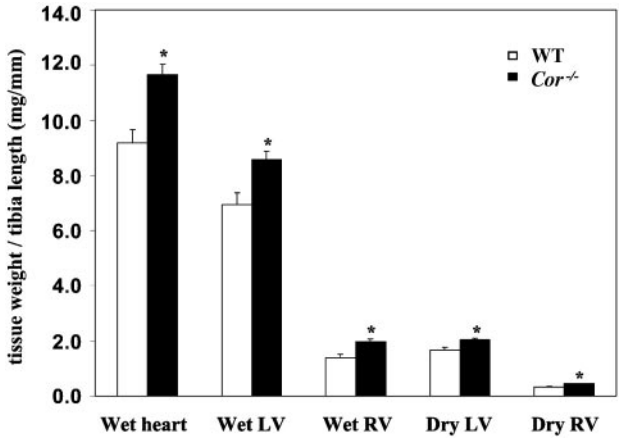

Fig. 4. Cardiac hypertrophy in *Cor*$^{-/-}$mice. *Cor*$^{-/-}$ mice had significant increases in total heart, LV and right ventricular weights when indexed to tibia length as compared to age-matched WT littermates. *, $P < 0.05$ vs. WT in the same group, by Student's *t* test.

genotypes. Histologic examination of cardiac sections from these animals found no overt pathological changes such as fibrosis and apoptosis in $Cor^{-/-}$ mice as compared with WT controls.

The diameter of individual cardiomyocytes in heart sections was also measured by computer-assisted image analysis. The mean cell diameter from $Cor^{-/-}$ mice appeared to be increased compared with that from WT mice (12.7 ± 0.2 μm vs. 12.4 ± 0.2 μm). The difference, however, did not reach statistical significance. Whole heart and individual chamber weights, indexed to tibia length, were also measured in older (>14 months) male mice (Fig. 4), which not only confirmed the increase in LV mass, as compared with WT age-matched littermates, but also revealed an increase in right ventricular weight. The increase in ventricular weight in $Cor^{-/-}$ mice was not due to increased water content because dry weight was also increased. Thus, our results indicate that deficiency in corin results in cardiac hypertrophy and decreased cardiac function in later life.

Discussion

ANP was discovered as a cardiac hormone by de Bold *et al.* (11) >20 years ago. Since then, the importance of the ANP-mediated pathway has been well established. In contrast, the enzyme(s) responsible for pro-ANP conversion remain poorly defined. Our recent *in vitro* studies indicate that the cardiac serine protease corin is a likely candidate of the missing pro-ANP convertase. To test this hypothesis, we created a corin-deficient mouse by homologous recombination. By HPLC and ELISA analyses, we found significantly increased levels of pro-ANP but no detectable ANP in atrial extracts from $Cor^{-/-}$ mice as compared with those in WT mice, indicating that the lack of corin prevented the conversion of pro-ANP to mature ANP in $Cor^{-/-}$ mice. i.v. injection of a recombinant-active corin transiently restored the production of biologically active ANP in $Cor^{-/-}$ mice. Thus, our results demonstrate that corin is the physiological pro-ANP convertase in mice and that, in its absence, no other enzymes can function in this role.

$Cor^{-/-}$ mice appear to develop normally. Histologic examinations of major organs such as brain, kidneys, lung, liver, and spleen revealed no abnormal phenotype. The finding is consistent with the studies of ANP-deficient and natriuretic peptide receptor A (NPRA)-deficient mice, indicating that the corin/ANP-mediated pathway is not essential for embryonic development and postnatal survival. $Cor^{-/-}$ mice exhibited increased body weight (11–15%) as compared with WT mice beginning at ≈4 months of age. These differences were similar in magnitude to that reported in $ANP^{-/-}$ mice (12), but the underlying mechanism is not clear. In principle, alterations of sodium homeostasis could increase extracellular fluid volume, leading to an increase in body weight. Future detailed analyses are needed to examine sodium retention and extracellular fluid volume in $Cor^{-/-}$ mice.

The ANP-mediated pathway plays an important role in regulating blood pressure. In mice, ANP deficiency or NPRA deficiency results in hypertension (13–15), whereas ANP or NPRA overexpression leads to hypotension (15, 16). We found that $Cor^{-/-}$ mice developed spontaneous hypertension with both elevated SBP and DBP, demonstrating that corin is critical in maintaining normal blood pressure. The blood pressure in $Cor^{-/-}$ mice was further enhanced with a high-salt diet, a similar phenotype observed in $ANP^{-/-}$ (13, 14) and $NPRA^{-/-}$ mice (15). Given the role of the ANP-mediated pathway in promoting salt excretion, it is expected that $Cor^{-/-}$ mice under a high-salt diet may have a lag in urinary salt excretion with an eventual return to balance. Such a phenomenon is observed in many forms of salt-sensitive hypertension (17). More detailed analysis of sodium balance will be necessary to evaluate sodium homeostasis in $Cor^{-/-}$ mice.

In addition to its role in blood pressure regulation, the ANP signaling pathway also has an antihypertrophic function in the heart. In experimental animal models, the ANP-mediated pathway has been shown to have a local antihypertrophic effect on cardiomyocytes that is independent of its systemic effect on blood pressure (12, 18–22). As measured by two-dimensional transthoracic echocardiography and heart weight, $Cor^{-/-}$ mice also develop cardiac hypertrophy. It remains to be determined whether the phenotype was caused primarily by the increase of blood pressure or the lack of local ANP in the heart in these animals. Nevertheless, our results suggest that corin deficiency or dysfunction in humans could contribute to heart disease. Most recently, polymorphisms in the corin gene have been identified that are associated with hypertension and cardiac hypertrophy in patients (D. Dries and A. Rame, personal communication). Further studies will help to verify the role of corin in heart disease.

In addition to the heart, corin mRNA was detected in the uterus from pregnant mice (2), suggesting a role of corin during pregnancy. We found that hypertension in $Cor^{-/-}$ females was exacerbated during pregnancy. Urinalysis of late-gestation $Cor^{-/-}$ females also revealed elevated levels of protein. Thus, corin-mediated pro-ANP processing appears to be a physiological mechanism to maintain normal blood pressure during pregnancy when significant hemodynamic changes occur. This hypothesis is supported by *de novo* placental pro-ANP synthesis (23–25), increased circulating ANP levels (26, 27), and tissue-specific NPR profile changes (28, 29) during pregnancy. In addition, secretion of paracrine factors from the fetus could potentially cross the placenta to influence maternal hemodynamics (30). Indeed, the trend toward decreased blood pressure takes place around the gestational timeframe when the embryonic heart and the circulatory system begin to develop, and corin, ANP, and NPRA are all expressed during this period (2, 31, 32). The importance of the ANP signaling pathway during pregnancy is underscored by reports of increased pro-ANP/ANP in patients with gestational hypertension, preeclampsia, or eclampsia. However, except for a few studies in which increased pro-ANP, but not ANP, was confirmed by HPLC-based methods (33), most studies used antibody-based methods, which do not discern between pro-ANP and ANP. Previous studies with ANP- and NPRA-deficient mice did not examine whether blood pressure is altered during pregnancy. Further studies are needed to assess the importance of corin-mediated pro-ANP processing in patients with pregnancy-related complications.

We thank M. Ferrell for assistance in cloning murine *corin*; R. Pagila for advice in RP-HPLC analysis; J. Vincelette and I. Cornelissen (University of California, San Francisco) for advice on blood pressure measurements; M. Schroeder, C. Almond, Drs. M. Halks-Miller, R. Meisner, and D. Fairchild for histopathology; and R. Fitch for advice on statistical analysis.

1. Levin, E. R., Gardner, D. G. & Samson, W. K. (1998) *N. Engl. J. Med.* **339,** 321–328.
2. Yan, W., Sheng, N., Seto, M., Morser, J. & Wu, Q. (1999) *J. Biol. Chem.* **274,** 14926–14935.
3. Hooper, J. D., Scarman, A. L., Clarke, B. E., Normyle, J. F. & Antalis, T. M. (2000) *Eur. J. Biochem.* **267,** 6931–6937.
4. Pan, J., Hinzmann, B., Yan, W., Wu, F., Morser, J. & Wu, Q. (2002) *J. Biol. Chem.* **277,** 38390–38398.
5. Yan, W., Wu, F., Morser, J. & Wu, Q. (2000) *Proc. Natl. Acad. Sci. USA* **97,** 8525–8529.
6. Wu, F., Yan, W., Pan, J., Morser, J. & Wu, Q. (2002) *J. Biol. Chem.* **277,** 16900–16905.
7. Knappe, S., Wu, F., Masikat, M. R., Morser, J. & Wu, Q. (2003) *J. Biol. Chem.* **278,** 52363–52370.
8. Corthorn, J., Cantin, M. & Thibault, G. (1991) *Mol. Cell Biochem.* **103,** 31–39.
9. Moreau, T., Brillard-Bourdet, M., Chagas, J. & Gauthier, F. (1995) *Biochim. Biophys. Acta* **1249,** 168–172.
10. Butz, G. M. & Davisson, R. L. (2001) *Physiol. Genomics* **5,** 89–97.
11. de Bold, A. J., Borenstein, H. B., Veress, A. T. & Sonnenberg, H. (1981) *Life Sci.* **28,** 89–94.

12. Feng, J. A., Perry, G., Mori, T., Hayashi, T., Oparil, S. & Chen, Y. F. (2003) *Clin. Exp. Pharmacol. Physiol.* **30,** 343–349.
13. John, S. W., Krege, J. H., Oliver, P. M., Hagaman, J. R., Hodgin, J. B., Pang, S. C., Flynn, T. G. & Smithies, O. (1995) *Science* **267,** 679–681.
14. John, S. W., Veress, A. T., Honrath, U., Chong, C. K., Peng, L., Smithies, O. & Sonnenberg, H. (1996) *Am. J. Physiol.* **271,** R109–R114.
15. Oliver, P. M., John, S. W., Purdy, K. E., Kim, R., Maeda, N., Goy, M. F. & Smithies, O. (1998) *Proc. Natl. Acad. Sci. USA* **95,** 2547–2551.
16. Steinhelper, M. E., Cochrane, K. L. & Field, L. J. (1990) *Hypertension* **16,** 301–307.
17. Ahn, D., Ge, Y., Stricklett, P. K., Gill, P., Taylor, D., Hughes, A. K., Yanagisawa, M., Miller, L., Nelson, R. D. & Kohan, D. E. (2004) *J. Clin. Invest.* **114,** 504–511.
18. Horio, T., Nishikimi, T., Yoshihara, F., Matsuo, H., Takishita, S. & Kangawa, K. (2000) *Hypertension* **35,** 19–24.
19. Silberbach, M. & Roberts, C. T., Jr. (2001) *Cell Signal* **13,** 221–231.
20. Knowles, J. W., Esposito, G., Mao, L., Hagaman, J. R., Fox, J. E., Smithies, O., Rockman, H. A. & Maeda, N. (2001) *J. Clin. Invest.* **107,** 975–984.
21. Kishimoto, I., Rossi, K. & Garbers, D. L. (2001) *Proc. Natl. Acad. Sci. USA* **98,** 2703–2706.
22. Holtwick, R., van Eickels, M., Skryabin, B. V., Baba, H. A., Bubikat, A., Begrow, F., Schneider, M. D., Garbers, D. L. & Kuhn, M. (2003) *J. Clin. Invest.* **111,** 1399–1407.
23. Huang, W., Lee, D., Yang, Z., Casley, D., Throsby, M., Copolov, D. L., Johnston, C. & Lim, A. T. (1992) *Endocrinology* **131,** 919–924.
24. Lim, A. T. & Gude, N. M. (1995) *J. Clin. Endocrinol. Metab.* **80,** 3091–3093.
25. Graham, C. H., Watson, J. D., Blumenfeld, A. J. & Pang, S. C. (1996) *Biol. Reprod.* **54,** 834–840.
26. Kristensen, C. G., Nakagawa, Y., Coe, F. L. & Lindheimer, M. D. (1986) *Am. J. Physiol.* **250,** R589–R594.
27. Chapman, A. B., Abraham, W. T., Zamudio, S., Coffin, C., Merouani, A., Young, D., Johnson, A., Osorio, F., Goldberg, C., Moore, L. G., *et al.* (1998) *Kidney Int.* **54,** 2056–2063.
28. Omer, S., Vaillancourt, P., Peri, K. G., Varma, D. R. & Mulay, S. (1997) *Am. J. Physiol.* **272,** F87–F93.
29. Vaillancourt, P., Omer, S., Deng, X. F., Mulay, S. & Varma, D. R. (1998) *Am. J. Physiol.* **274,** E52–E56.
30. Takeda, T. (1964) *Jpn. Circ. J.* **28,** 55–63.
31. Zeller, R., Bloch, K. D., Williams, B. S., Arceci, R. J. & Seidman, C. E. (1987) *Genes Dev.* **1,** 693–698.
32. Brown, J. & Zuo, Z. (1995) *Am. J. Physiol.* **269,** E253–E268.
33. Pouta, A. M., Vuolteenaho, O. J. & Laatikainen, T. J. (1997) *Obstet. Gynecol.* **89,** 747–753.